

Article

# Complex Microlandscape as a Structural Unit of the Study of Spatiotemporal Development of an Ombrotrophic Suboceanic Bog

Tamara Ponomareva , Ivan Zubov , Anastasiya Shtang, Alexander Orlov and Svetlana Selyanina

N. Laverov Federal Center for Integrated Arctic Research, Ural Branch of the Russian Academy of Sciences, Nokolsky Avenue, 20, Arkhangelsk 163000, Russia

\* Correspondence: [ponomtamara@gmail.com](mailto:ponomtamara@gmail.com) or [gumin@fciaarctic.ru](mailto:gumin@fciaarctic.ru)

**Abstract:** Ombrotrophic suboceanic bogs are distinguished by a high diversity of complex microlandscapes within the bog massif. Each complex microlandscape is a separate intrabog ecosystem with a specific set of parameters and relationships. This study aims to assess the specifics of the characteristics and parameters of the complex microlandscapes as part of an ombrotrophic suboceanic Sphagnum bog and as stages of bog morphogenesis, and to establish the internal relationships and their relationship with external environmental factors. A comprehensive multidisciplinary approach was used to assess the functioning of the complex microlandscapes. It was found that the relationship with the air temperature is closer than with the bog water table dynamics. It was shown that the morphometric parameters of perennial dwarf shrubs can serve as indicators of the stages of development of bogs. The processes of the self-regulation of complex microlandscapes are weakened with the age of the complex microlandscape, as evidenced by an increase in the amplitude of temperature fluctuations and the level of bog waters, as well as the key physicochemical parameters of the peat deposit. This leads to a gradual, slow reorientation of the physicochemical processes occurring in the deposit, from the deposition of organic matter to the decomposition of peat biomass.

**Keywords:** bog ecology; bog plant communities; physico-chemical parameters of peat deposit; bog microclimate



**Citation:** Ponomareva, T.; Zubov, I.; Shtang, A.; Orlov, A.; Selyanina, S. Complex Microlandscape as a Structural Unit of the Study of Spatiotemporal Development of an Ombrotrophic Suboceanic Bog. *Quaternary* **2024**, *7*, 19. <https://doi.org/10.3390/quat7020019>

Academic Editor: Bas Van Geel

Received: 13 November 2023

Revised: 4 April 2024

Accepted: 12 April 2024

Published: 15 April 2024



**Copyright:** © 2024 by the authors. Licensee MDPI, Basel, Switzerland. This article is an open access article distributed under the terms and conditions of the Creative Commons Attribution (CC BY) license (<https://creativecommons.org/licenses/by/4.0/>).

## 1. Introduction

Boreal forests are the second largest forest biome after tropical forests, covering 11.4 million km<sup>2</sup> [1]. The basis of the ecological skeleton of the boreal biome is coniferous forests and wetlands, which are parts of a single system that are in constant spatiotemporal dynamics and exhibit a mutual influence upon one another [2]. Wetlands are an important component for maintaining ecological balance; they form a natural network, contributing to the formation of a rather heterogeneous and fragmented structure of forest cover in the boreal forest zone, which significantly increases the stability of forest-bog ecosystems [3–7]. Boreal forests and wetlands play a critical role in the global carbon cycle. Moreover, 50 to 73% of the carbon sequestration in the boreal biome falls on the wetlands [8]. Ombrotrophic convex Sphagnum bogs occupy up to 67% of the wetlands in the boreal biome [8,9]. The north of the boreal forest zone is the optimal environment for such type of bogs; large bog massifs (up to 20 thousand ha) and extensive systems of bog massifs form here [10–14].

The emergence of European boreal bogs is associated with the end of the last glaciation (20–9 thousand years ago) [15–17]. The formation of bogs began in the glacial depressions of the Late Valdai glaciation and associated dammed lakes, when the territory lost its ice and water [18]. The specificity of bog formation in the European north lies in the fact that it began immediately after the retreat of the glacier and developed evenly over vast areas of flat interfluvies. In the Subboreal period (4500–2500 years ago), oligotrophic processes in the north of the European part of the boreal biome reached a maximum; hummock–hollow and

hummock–pool complexes began to combine into bog systems, which were accompanied by an active accumulation of weakly decomposed ombrotrophic peat. In the Subatlantic period (from 2500 years ago to the present), bog systems formed in their modern form with well-differentiated hummock–hollow, hummock–pool–hollow, and hummock–pool complex microlandscapes with secondary lakes [14,19–22].

Ombrotrophic boreal Sphagnum bogs are distinguished by a high diversity of plant complexes within the bog massif. At the same time, they are an example of a complex autonomous self-developing paragenetic landscape where adjacent actively-interacting plant complexes have a common origin and development with a material and energy cycle that is practically independent of external conditions [23]. The supply of energy in the form of solar radiation and precipitation are the external factors that affect the development and existence of ombrotrophic bogs [24]. In a dynamic aspect, convex ombrotrophic bogs refer to the final stage of bog formation, where complexes with regressive phenomena (ridge–pool complexes and denuded ridges covered with lichens) are expressed [10,25]. This fact allows the consideration of convex ombrotrophic bogs as wetlands with the most pronounced and well-established mechanisms of functioning.

Hummock–pool–hollow bog complexes growing from the center in a distal direction are the most common type of convex ombrotrophic bog in the boreal forest zone [17,26]. The stages of bog development can be traced most clearly in this type of ombrotrophic bog. The morphological structure is clearly differentiated within the actively functioning ombrotrophic bog with a convex surface [27]. The morphogenetic row of an ombrotrophic bog development is as follows: a marginal swampy pine forest—a hummock–lawn–hollow complex (the formation of hummocks is at the initial stage, there is no orientation of the hummocks relative to the directions of the largest surface runoff)—a formed hummock–hollow complex (a hummock–hollow microrelief with emerging secondary lakes and a concentric pattern of hummocks)—and a hummock–pool complex. The cyclic lenticular “regeneration complex” model indicates the existence of such a morphogenetic series [28].

Recent research is focused on studying the relationship between biogenic cycles and greenhouse gas emissions with individual elements of bog ecosystems, most often with microtopography, the composition and structure of plant communities, the level of bog waters, etc. [25,29–31]. However, nowadays, a comprehensive, multidisciplinary approach is needed to assess the functioning of ecosystems [32]. Each complex microlandscape is a separate intrabog ecosystem with a specific set of parameters and relationships. Comprehensive studies of these intrabog ecosystems are needed to establish their contribution to the biogenic cycles of the bog in the spatial aspect. In the temporal aspect, complex microlandscapes should be considered as the stages of the morphogenetic development of the bog. This will enable us to not only establish the specifics of the ongoing processes at the present stage of development, but also to restore the mechanisms of biogenic cycles since the formation of the bog. Understanding the mechanisms of biogenic cycles at each historical stage of bog development and the factors that shift the established equilibrium towards the next morphogenetic stage will be useful for the scientifically based restoration of ombrotrophic bogs.

The hypothesis of the study is that complex microlandscapes, as separate stages of bog morphogenesis, are characterized by a specific set of parameters and characteristics of their components that regulate biogenic cycles. This is important both for a retrospective analysis and for establishing directions for the transformation of the organic matter cycle in the future under the influence of changing climatic conditions.

To confirm the hypothesis, it is necessary to:

- (1) Establish the specificity of the characteristics and parameters of the components of complex microlandscapes;
- (2) Establish specific internal relationships for complex microlandscapes;
- (3) Establish specific relationships between complex microlandscapes and environmental factors.

## 2. Materials and Methods

### 2.1. Study Area

The Arkhangelsk region is one of the largest peatland areas in European Russia. Peatlands occupy up to 50% of the terrestrial area, especially on the north boundary of the boreal forest distribution. The study area ( $64^{\circ}18'54''$  N;  $40^{\circ}41'14''$  E; 62 m above sea level) is located in the highly waterlogged watershed of the Severnaya Dvina river, near the city of Arkhangelsk, 55 km southward of the Dvina bay of the White Sea (the southern inlet of the Barents Sea). The climate of the study area is moderate continental subarctic with a prominent marine influence (the Köppen–Geiger climate classification is Dfb). The annual mean temperature is  $+2.3$  °C (the coldest month is January ( $-11.2$  °C); the warmest month is July ( $17.3$  °C)). The annual precipitation is 672 mm/yr (the greatest in August—84 mm; the least in February—32 mm). Slightly more than half of the annual precipitation (about 350 mm) falls during the growing season. The duration of snow cover is about 136 days; the growing season is about 100 days [33].

The study site “Ilasskoe Bog” is a vast complex of bogs, predominantly ombrotrophic (Figure 1), with a square area of more than 90 km<sup>2</sup> (the complex is 17 km in length and 3.8 km in width) [34]. This is a representative of European suboceanic *Sphagnum* raised bogs. Such bogs are characterized by an eccentric, slightly convex surface (the center is 1–3 m above the surface) and a slight slope towards the water intake [35]. The peat deposit consists of slightly decomposed high-moor peat lying directly on the clayey and loamy moraine. Bedrocks are represented by layered clays and sandstones. The mean depth of the peat deposit is 3.0–3.5 m; the greatest depth is about 6.0–8.0 m.

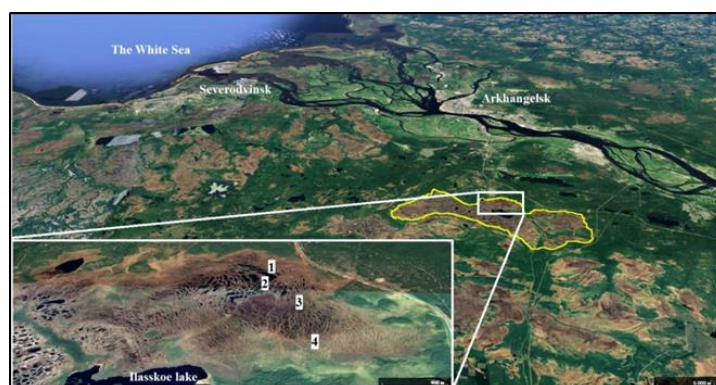


**Figure 1.** General location of the complex of bogs “Ilasskoe Bog”. Study sites: 1—hummock–pool complex; 2—hummock–pool–hollow complex; 3—hummock–hollow complex; 4—lawn complex. Modified from [36].

The studied bog massif has an area of 595 ha and is an ombrotrophic flat-convex mesolandscape with well-differentiated microtopographic complexes (complex microlandscapes): hummock–pool (HP), hummock–pool–hollow (HPH), hummock–hollow (HH), and lawn (L) (Figure 2). The vegetation of the studied bog massif is characteristic of boreal ombrotrophic bogs. The hummock–hollow–pool pattern dominates the studied bog massif. It forms the central part of the bog massif. Here, hummocks with pine, dwarf shrub and *Sphagnum* alternate with secondary lakes (the water surface area is about 0.001–0.002 km<sup>2</sup>) [34]. On the hummock–hollow microlandscape, pine-dwarf-shrub-*Sphagnum* hummocks alternate with *Scheuchzeria-Sphagnum* and sedge-*Sphagnum* hollows. Hummocks are arranged in a characteristic concentric pattern perpendicular to runoff lines. Lawns are presented by *Sphagnum*-cotton grass-shrub flat carpets without a tree layer, somewhere with weakly developed dwarf-shrub-*Sphagnum* hummocks not oriented towards run-off lines.

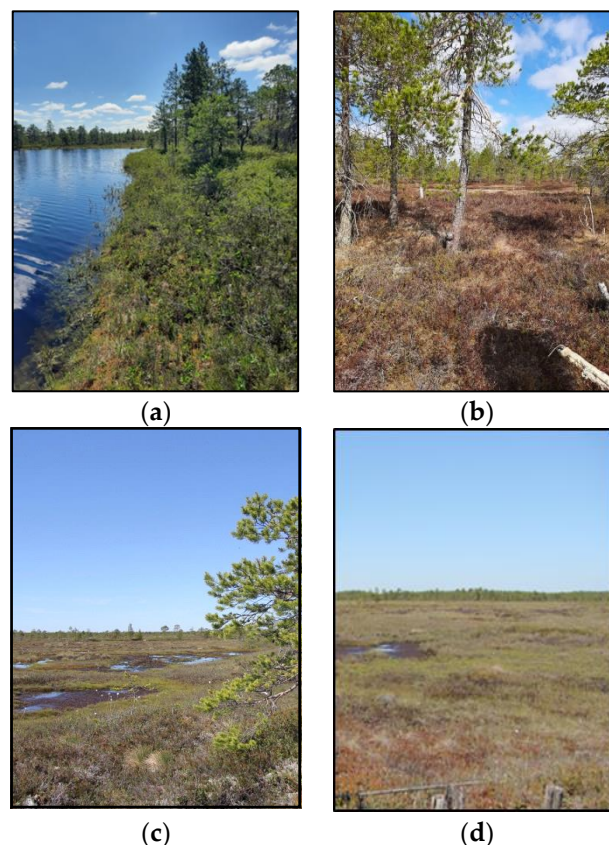


**Figure 2.** An overall view of the studied complex microlandscapes: (a) HP (hummock–pool complex); (b) HPH (hummock–pool–hollow complex); (c) HH (hummock–hollow complex); (d) L (lawn).

*Sphagnum* mosses are ecosystem engineers and environment-forming species of boreal ombrotrophic bogs. The Ilaskoe bog hummocks are dominated by *Sphagnum* species adapted to low bog water levels. *Sphagnum fuscum* (Schimp.) Klinggr. and *Sphagnum capillifolium* (Ehrh.) Hedw. grow on the elevated forms of nanorelief; *Sphagnum angustifolium* (Russ.) C. Jens. grows in less dry sites between the elevated forms of nanorelief. Large *Sphagnum papillosum* Lindb. plants grow along the edges of hollows and lawns. In hollows and on lawns, the species composition of *Sphagnum* mosses is represented by *Sphagnum jensenii* H. Lindb., *Sphagnum lindbergii* Schimp. ex Lindb., *Sphagnum majus* (Russ.) C. Jens., *Sphagnum balticum* (Russ.) Russ. ex C. Jens. In watered hollows and on the edges of the pools, *Cuspidata* is added to the species of the section *Sphagnum cuspidatum* Ehrh. et Hoffm. Depressed hollow species of *Sphagnum* mosses are found in some small areas of degraded hollows.

## 2.2. Materials and Methods

The vegetation study was carried out with a complete description of the living vegetation cover and the tree layer within the selected study sites on each complex microlandscape [37]. Studies were carried out using the method of eye estimation of projective cover and the abundance of plant species. The species of vascular plants were determined according to the reference [38]; the mosses were determined according to the papers [39,40]. Morphometric indicators of the tree layer were determined by the methods of visual taxation ( $n = 100$ ) [41]. The height of the trees was determined using the altimeter Haglof EC II D (Haglof, Långsele, Sweden); the diameter of the trees at breast height was measured using the measuring fork Haglof Mantax Blue (Haglof, Långsele, Sweden). The crown density was determined using the route method. The age of the trees on the study sites was determined using the increment borer Haglof (Haglof, Långsele, Sweden), followed by

a manual calculation of the number of annual rings using the binocular microscope Altami SM0745 (Altami, St. Petersburg, Russia).

The air temperature during the growing season 2022 (May to October) was evaluated using the combined thermohygrometer-light intensity meter-UV-radiometer “TKA-PKM-42” (LTD Scientific and Technical Enterprise “TKA”, St. Petersburg, Russia). The temperature regime of the plant cover and peat deposit at different depths was evaluated using the loggers DS1921G-F5 (Thermochron, Sydney, Australia). Precipitation data were obtained from the nearest weather station. The dynamics of the bog water levels were studied in hydrological wells with a diameter of 110 mm with a recess into the mineral layer. Bog water level measurements were carried out once every 14 days throughout the warm season of 2022 (May–October).

The evaluation of ORP (oxidation reduction potential) of the peat deposit layers was made in situ using direct potentiometry with the original probe measuring devices developed by the authors, with no extraction of peat samples and excluding its oxidation. The temperature of each layer of the peat deposit was also recorded. Field pH and total mineralization determinations were also performed using the potentiometric method in pore water squeezed from the investigated peat layers. The methodology of ORP and pH measuring and converting the resulting ORP data in  $Eh_4$  (to standard conditions:  $t = 25\text{ }^{\circ}\text{C}$  with  $\text{pH} = 4.0$ ) is presented in more detail in previous studies [42,43].

Peat sampling was carried out via layer-by-layer drilling using a peat sampler of stainless steel P 04.09 (EIJKELKAMP, Giesbeek, The Netherlands). The diameter of the peat core was 52 mm. Peat cores ( $n = 10$ ) were collected randomly in each study site with 10 cm sampling intervals through the depth of the deposit.

Plant residues and the degree of peat decomposition were identified according to [44] using an Altami Bio 2 microscope completed with an Ucmos 03100KPA digital camera and Altami Software.

The radiocarbon dating of peat samples was performed in the laboratory “Geomorphological and paleogeographic research of polar regions and the World Ocean” of SPbSU by means of a scintillation account on the low-background liquid scintillation spectrometer “Quantulus 1220” (PerkinElmer, Buckinghamshire, UK) according to the standard method [45]. Based on the results of measuring the velocities of the sample, the background and standard, radiocarbon, and calendar age were calculated using the “OxCal” calibration program and the IntCal 20 calibration curve [46].

The basic statistics (namely, average value, minimum and maximum values, and standard deviation) were calculated for the obtained data using the package “Data Analysis” for MS Excel. The differences between the study sites were determined using the Mann–Whitney U-criterion and the Kruskal–Wallis criterion (SPSS) [47]. The relationship between the studied parameters was established by calculating the Spearman rank correlations (SPSS). The study sites’ data were analyzed using hierarchical clustering. The method of between-group linkage was chosen as the clustering method. The list of variables for clustering included the characteristics of the upper layers of peat deposits and the vegetation cover of the study sites: temperature, mineralization, pH, and electrical conductivity in the peat layer of 0–10 cm, as well as the protective cover of vascular plants and mosses. The data analyzed using cluster analysis were transformed into a single z-scale due to differences in measurement scales. The distance between the cases was measured using the squared Euclidean distance. The results of the analysis were presented as a dendrogram.

### 3. Results

#### 3.1. Microclimate Characteristics

Data from the nearest weather station were used to characterize the local climate from May to October 2022. The local climate was characterized by a mean air temperature of  $15.1 \pm 7.6\text{ }^{\circ}\text{C}$ . The maximum air temperature was  $30.5\text{ }^{\circ}\text{C}$  and it was observed on 12 July; the minimum air temperature was  $0.2\text{ }^{\circ}\text{C}$  below zero and was observed on 26 October (Figure 3a). The precipitation was 342 mm for the period of May–October 2022. The highest

precipitation was 120 mm in July. The maximum (136 mm) is due to the inclusion of precipitation for the preceding winter period, because it enters the peat deposit during the active thawing in April (Figure 4). The mean daily precipitation was  $1.84 \pm 2.85$  mm. Here the data, and further data, are presented in the form of mean value  $\pm$  standard deviation. The maximum daily precipitation was 16.9 mm on July 30th. The dynamics of air temperature and living vegetation cover at the study sites are shown in Figure 3.

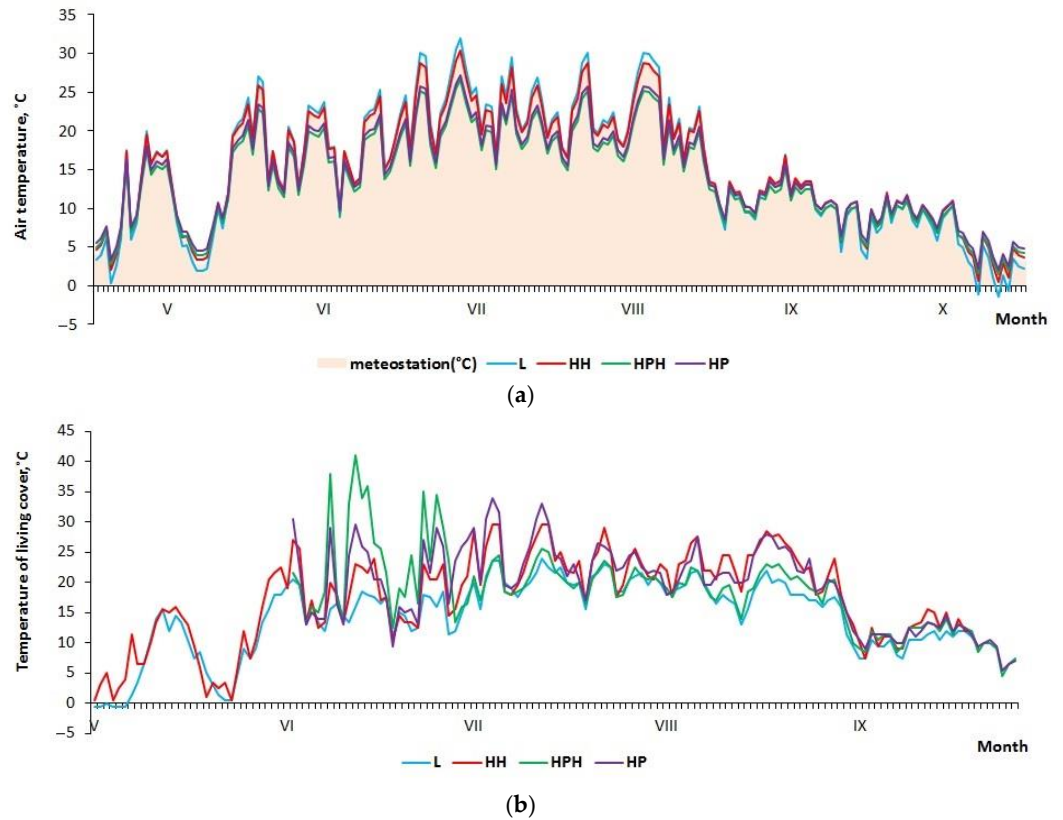


**Figure 3.** The temperature of the air (a) and living vegetation cover (b) during the warm season of 2022 at the study sites: HP (hummock–pool complex); HPH (hummock–pool–hollow complex); HH (hummock–hollow complex); L (lawn).

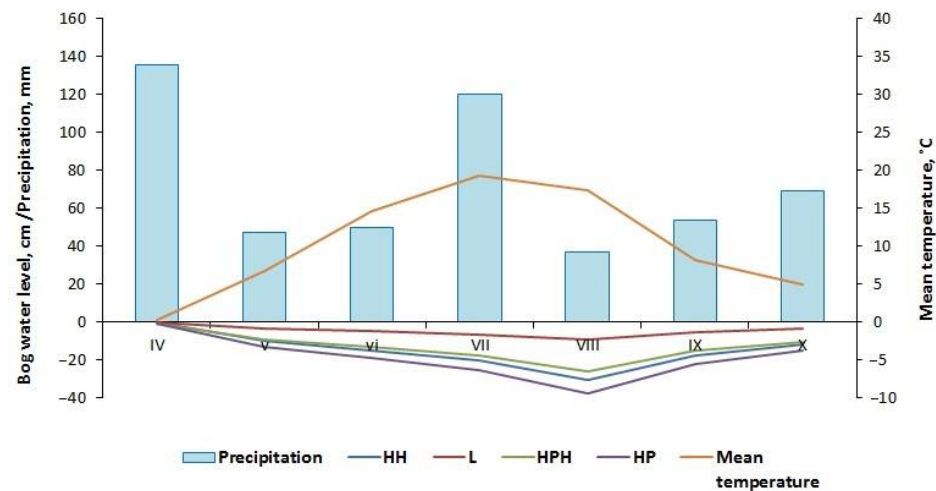


**Figure 4.** The bog water levels, mean monthly precipitation, and air temperature during the warm season of 2022.

The course of air temperatures at the studied sites, in general, repeats the course of air temperatures at the weather station. The mean temperature for the warm season on site L was  $15.2 \pm 8.2$  °C; on site HH it was  $15.3 \pm 7.4$  °C; on site HPH it was  $13.9 \pm 6.2$  °C; and on site HP it was  $14.5 \pm 6.2$  °C. The maximum air temperature in the investigated areas was recorded on the same day as at the weather station—the 12th of July. It was 32 °C (at site L); 30.4 °C (at site HH); 26.5 °C (at site HPH); 27.2 °C (at site HP). The minimum air temperature at the study sites was recorded on October 26th, similar to the data from the weather station, and was: 1.4 °C below zero (at site L); 0.4 °C (at site HH); 1.5 °C (at site HPH); 2.0 °C (at site HP).

The dynamics of the temperature of the living vegetation cover (Figure 3b) is similar to the dynamics of the air temperature at the studied sites. The mean temperatures of the living vegetation cover for the warm season at the study sites were:  $14.5 \pm 6.1$  °C (L);  $17.4 \pm 7.3$  °C (HH);  $18.6 \pm 6.6$  °C (HPH);  $19.7 \pm 6.6$  °C (HP). The maximum living vegetation cover temperature (according to data from temperature loggers) at the study sites was also observed on July 12th: 24.0 °C (L); 29.5 °C (HH); 41.0 °C (HPH); 34.0 °C (HP). The minimum living vegetation cover temperature was recorded in the first week of May for all sites (0.5 °C below zero).

The mean bog water level during the warm period was:  $-4.6 \pm 2.9$  cm (at site L);  $-15.0 \pm 9.5$  cm (at site HH);  $-13.2 \pm 7.7$  cm (at site HPH);  $-18.9 \pm 11.3$  cm (at site HP) (Figure 4). At the beginning of the warm season, the bog water level was close to the ground surface level on all sites. In August, bog water was lowered to its maximum depth:  $-9.4$  cm (L);  $-30.0$  cm (HH);  $-25.8$  cm (HPH);  $-37.4$  cm (HP). By the end of the warm season, bog water levels gradually rose closer to the ground surface. At the end of October, bog water levels were:  $-3.6$  cm (L),  $-11.8$  cm (HH),  $-10.6$  cm (HPH), and  $-15.1$  cm (HP).

### 3.2. Vegetation

The tree layer on the studied bog is represented by the bog forms of *Pinus sylvestris* L. growing on the hummocks. The characteristics of the tree layer are given in Table 1.

**Table 1.** The characteristics of the tree layer at the study sites.

Study Site	Tree Layer Composition	Age of the Trees, Years	Mean		Relative Crown Density	Dominant Ecological Form of Pine
			Height, m	Diameter, cm		
Lawn (L)	-	-	-	-	-	-
Hummock–hollow complex (HH)	<i>Pinus sylvestris</i> L.	$51.08 \pm 19.53$ <sup>*ab</sup>	$2.44 \pm 1.38$ <sup>cd</sup>	$4.34 \pm 3.50$ <sup>ef</sup>	$0.30 \pm 0.28$	<i>f. willkommii</i>
Hummock–pool–hollow complex (HPH)	<i>Pinus sylvestris</i> L.	$211.5 \pm 71.02$ <sup>a</sup>	$3.26 \pm 1.36$ <sup>c</sup>	$8.45 \pm 6.41$ <sup>e</sup>	$0.50 \pm 0.40$	<i>f. litwinowii</i>
Hummock–pool complex (HP)	<i>Pinus sylvestris</i> L.	$145.30 \pm 33.30$ <sup>b</sup>	$3.07 \pm 1.45$ <sup>d</sup>	$7.29 \pm 6.86$ <sup>f</sup>	$0.54 \pm 0.43$	<i>f. litwinowii</i>

\* Data presented as mean value  $\pm$  standard deviation. The same code letter indicates statistically significant differences between study sites in studied parameters (U Mann–Whitney test,  $p < 0.05$ ).

At the lawn site, Scots pine trees are sporadic on emerging hummocks; living specimens are severely depressed or absent. The tree layer at the hummock–hollow complex microlandscape is characterized by the lowest crown density (it does not exceed  $0.30 \pm 0.28$ ) and tree morphometry (mean height is  $2.44 \pm 1.38$  m, mean diameter  $4.34 \pm 3.50$  cm). On the hummocks of the hummock–pool complex microlandscape, Scots pine tree stands are the densest (the mean crown density is  $0.54 \pm 0.43$ ), with a mean height of  $3.07 \pm 1.45$  m and the mean diameter of  $7.29 \pm 6.86$  cm. The study site at the hummock–pool–hollow complex microlandscape is characterized by a crown density of  $0.50 \pm 0.40$ , with the maximal mean height and diameter of the Scots pine trees ( $3.26 \pm 1.36$  m and  $8.45 \pm 6.41$  cm, respectively). The studied tree stands differ in the predominant ecological form of Scots pine. The hummock–hollow complex microlandscape is characterized by the predominance of the ecological form of *Pinus sylvestris* f. *willkommii*, while the tree stands at the hummock–pool and hummock–pool–hollow complex microlandscapes are predominated by the ecological form of *Pinus sylvestris* f. *litwinowii*. A shrub layer is absent at all study sites.

The study site L is characterized by a continuous moss cover with 100% projective cover composed of hygrophytic and hydrophytic species of *Sphagnum* mosses, among which there are small plants of *Andromeda polifolia* L. and hygrophilous herbs *Eriophorum vaginatum* L., *Rhynchospora alba* (L.) Vahl., *Scheuchzeria palustris* F. Muell. with a low projective coverage (Table S1). It should be noted that *Oxycoccus* spp. and *Drosera* spp. are widespread in the studied bog and also found in all complex microlandscapes. On the forming hummocks of the study site L, the living vegetation cover is unevenly developed. On some hummocks, the dwarf shrub layer is developed quite well and represented by several dominant species such as *Calluna vulgaris* (L.) Hill (mean plant height  $21.9 \pm 5.86$  cm); *Empetrum hermaphroditum* Lange ex Hagerup (mean plant height  $12.1 \pm 4.91$  cm); *Ledum palustre* L. (mean plant height  $24.6 \pm 6.83$  cm); and *Vaccinium uliginosum* L. (mean plant height  $17.4 \pm 2.88$  cm) with a projective cover of 10–15%. The mean heights of the dominant species of dwarf shrubs at the study sites are shown in Figure 5.

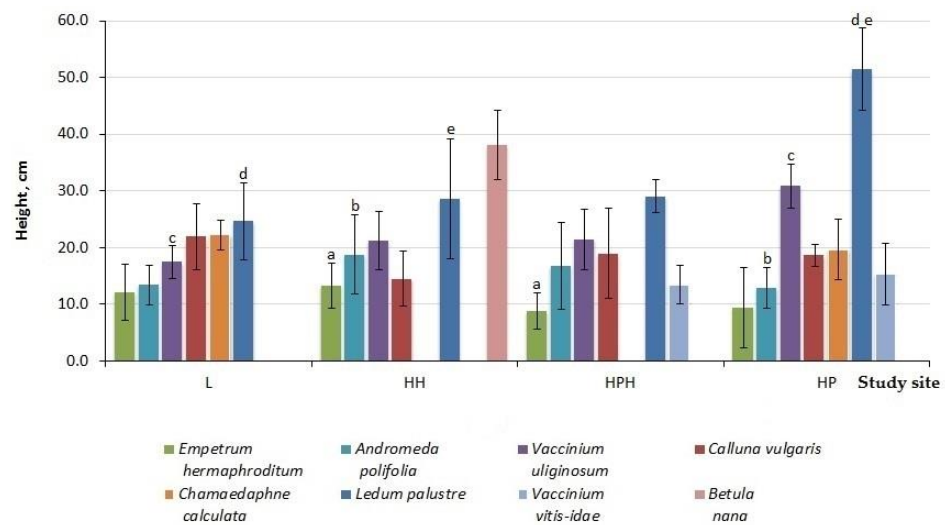


**Figure 5.** The mean height (the bars indicating the standard deviation value) of dominating shrubs at the study sites: HP (hummock–pool complex); HPH (hummock–pool–hollow complex); HH (hummock–hollow complex); L (lawn). The same code letter on the diagram bar indicates statistically significant differences in the height of the shrub species (U Mann–Whitney test,  $p < 0.05$ ).

The moss–lichen layer at the study site L consists of *Sphagnum* and green mosses (the projective covering is 30 and 50%, respectively), as well as *Cladonia* spp. lichens (the projective coverage is up to 5%) (Figure 6). There are hummock communities with *Andromeda polifolia* L. (mean height of plants  $13.4 \pm 3.50$  cm) with a 15% projective cover, in which the participation of other dwarf shrubs is minimal. The presence of *Rubus chamaemorus* L. was noted on all hummocks; its projective coverage reaches 30% on hummocks with a developed dwarf shrub layer. On some hummocks, the projective cover of the dominant species of shrubs is reduced to 5%, and the moss layer formed only by *Sphagnum* mosses, on the contrary, is strongly developed: its projective cover is 100%.

At the hummock–hollow complex microlandscape (HH), the hummocks and hollows are well differentiated. Degraded hollows with no plant cover appear in the central part of the study site HH. The hummocks are dominated by shrubs *Andromeda polifolia* L. (mean height of plants  $18.7 \pm 6.96$  cm), *Calluna vulgaris* (L.) Hill (mean height of plants  $14.5 \pm 4.81$  cm), *Empetrum hermaphroditum* Lange ex Hagerup (mean height of plants  $13.3 \pm 4.03$  cm), *Ledum palustre* L. (mean height of plants  $28.5 \pm 10.56$  cm), *Vaccinium uliginosum* L. (mean height of plants  $21.2 \pm 5.14$  cm), *Betula nana* L. (mean height of plants:  $38.1 \pm 6.05$  cm). The projective cover of dwarf shrub dominants ranges from 5 to 20%; the projective cover of heather reaches 70% in some communities. The projective coverage of *Rubus chamaemorus* L. is 5–20% on the hummocks. The projective cover of the moss layer, consisting of *Sphagnum* mosses with inclusions of true mosses, reaches 60%. *Cladonia* spp.

lichens are adjacent to the *Sphagnum* mosses with a projective cover up to 20%. On the site (HH), the hollows with *Eriophorum vaginatum* L. and *Scheuchzeria palustris* F. Muell. are common. The projective cover on the *Sphagnum* mosses is 100% in such hollows. In degraded hollows, there are quite extensive areas of naked black peat, which decrease the projective cover of *Sphagnum* mosses by up to 20–40%. *Rhynchospora alba* (L.) Vahl. with a projective cover of 15%, is adjacent to the few *Eriophorum vaginatum* L. and *Scheuchzeria palustris* F. Muell. plants; it is a notable dominant of the herbaceous layer. In heavily watered hollows, *Sphagnum* shoots are arranged in water more sparsely than in hollows, where the bog water level is under the heads of *Sphagnum* plants. Therefore, the projective cover of *Sphagnum* mosses in watered hollows is close to 90%. *Scheuchzeria palustris* F. Muell. is quite abundant in hollows with a projective cover of 5%.

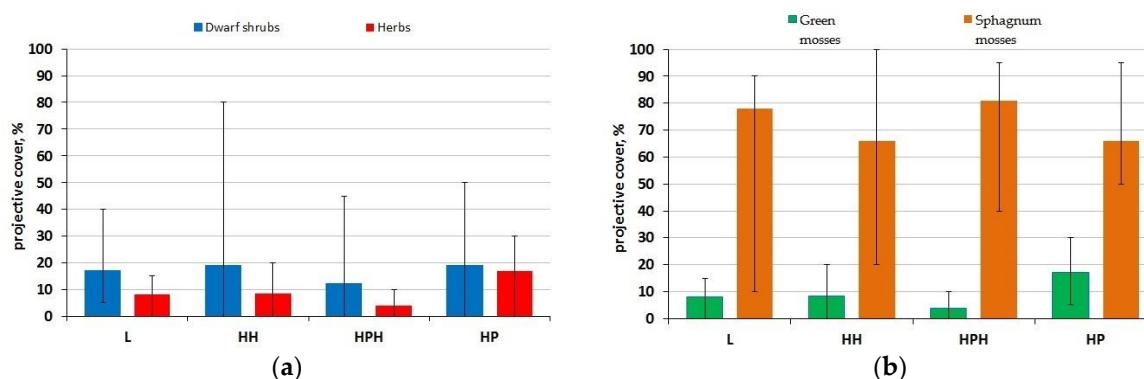


**Figure 6.** The projective cover of the main vegetation groups at the study sites: HP (hummock–pool complex); HPH (hummock–pool–hollow complex); HH (hummock–hollow complex); L (lawn): (a) dwarf shrub-herbal layer; (b) moss cover. There are no statistically significant differences between the study sites for projective cover of plant groups (U Mann–Whitney test,  $p < 0.05$ ).

On the hummocks of the studied hummock–pool–hollow complex microlandscape (HPH), the shrubs are numerous and varied. They are: *Andromeda polifolia* L. (mean plant height  $16.7 \pm 7.65$  cm), *Calluna vulgaris* (L.) Hill (mean plant height  $18.9 \pm 7.95$  cm), *Empetrum hermaphroditum* Lange ex Hagerup (mean plant height  $8.7 \pm 3.15$  cm), *Ledum palustre* L. (mean plant height  $29.0 \pm 2.92$  cm), *Vaccinium uliginosum* L. (mean height of plants  $21.4 \pm 5.30$  cm); also, *Vaccinium vitis-idea* L. appears (mean height of plants  $13.4 \pm 3.36$  cm). The projective cover of the dominant species is 5–10%. *Rubus chamaemorus* L. is present in the vegetation cover with a projective cover of 10%. The moss layer of the hummocks is formed by *Sphagnum* and green mosses, whose projective coverage is 30 and 10%, respectively. Lichens of the genera *Cladonia* and *Cetraria* are sporadic. On the edges of the hummocks, the shrubs have an extremely low projective cover, but patchy *Andromeda polifolia* forms communities with a projective cover of up to 15%. In the areas where the bog rosemary has abundant growth, *Rubus chamaemorus* L. has a projective coverage of 10%. The herbal layer is also represented by *Eriophorum vaginatum* L. and *Trichophorum cespitosum* (L.) Hartm. The percentage of the projective cover of *Sphagnum* mosses on the edges of the hummocks is much higher than in the central parts and reaches 80–95%. *Andromeda polifolia* L., *Rhynchospora alba* (L.) Vahl., and *Scheuchzeria palustris* F. Muell. with a low percentage of projective cover grow in hollows. *Scheuchzeria palustris* F. Muell. does not grow on the edges of the hollows, but there are *Carex limosa* L. and *Eriophorum vaginatum* L. The projective coverage of *Sphagnum* mosses in the hollows is 95%.

The degraded hollow plant community is dominated by *Eriophorum vaginatum* L. (the projective cover is 20%) and *Rhynchospora alba* (L.) Vahl. (the projective cover is near 5%); also, *Scheuchzeria palustris* F. Muell. appears. *Sphagnum* mosses form a layer with a projective cover of 50%; the rest of the space is occupied by bare peat.

The shrub layer of hummocks in the hummock–pool complex microlandscape (HP) is characterized by a relatively rich species-set. Dominant species *Calluna vulgaris* (L.) Hill

(mean plant height  $18.6 \pm 1.90$  cm), *Empetrum hermaphroditum* Lange ex Hagerup (mean plant height  $9.40 \pm 7.00$  cm), *Ledum palustre* L. (mean plant height  $51.4 \pm 7.30$  cm), *Vaccinium uliginosum* L. (mean plant height  $30.8 \pm 3.80$  cm), and *Vaccinium vitis-idea* L. (mean plant height  $15.2 \pm 5.50$  cm) have a projective coverage of 5 to 20%. *Andromeda polifolia* L. (mean plant height  $12.9 \pm 3.50$  cm), *Chamaedaphne calyculata* (L.) Moench (mean plant height  $19.6 \pm 5.40$  cm), and single plants of *Vaccinium myrtilloides* L. appear on the hummocks. The projective cover of *Rubus chamaemorus* L. is 30%. *Eriophorum vaginatum* L. is found. In the moss–lichen layer, the projective cover of true mosses is larger than the projective cover of *Sphagnum* mosses (40% and 20%, respectively) and the lichens *Cladonia* spp. and *Cladonia* spp. are found. *Vaccinium* spp. plants are absent along the edges of the hummocks. In the hollows, where *Sphagnum* mosses have a projective cover of 95%, the herbal layer is dominated by *Scheuchzeria palustris* F. Muell. (projective cover of 5%). *Rubus chamaemorus* L., *Eriophorum vaginatum* L., and *Andromeda polifolia* L. plants appear in *Scheuchzeria palustris* F. Muell. communities.

### 3.3. Peat Deposit Characteristics

#### 3.3.1. Age, Botanical Composition, and Degree of Decomposition of Peat

It was determined that the maximum depth of the peat deposit is 5.90 m (study site HP) in the central part of the studied bog massif. It gradually decreases towards the edge of the bog massif: to 3.20–3.50 m at the study sites HH and HPH, and further to 2.40–2.60 m at the study site L. The results of the absolute age of the peat deposit determined using radiocarbon analysis are presented in Table 2.

**Table 2.** Results of the determination of the absolute age of peat deposits using the radiocarbon method.

Study Site	Sample Name	Peat Depth, m	Radiocarbon Age, yr	Calibrated Age, cal.yr BP
L	LU-10913 *	2.40–2.60	$4990 \pm 80$	$5740 \pm 90$
HH	LU-10912 *	3.30–3.50	$5780 \pm 90$	$6580 \pm 110$
HPH	LU-10911 *	3.20–3.40	$5940 \pm 80$	$6780 \pm 100$
HP	LU-10910 *	5.80–6.00	$9280 \pm 90$	$10,460 \pm 130$

\* The samples for radiocarbon dating were extracted from the base of the peat deposits.

The absolute age of the peat deposits at the study sites ranges from  $5740 \pm 90$  cal.yr BP to  $10,460 \pm 130$  cal.yr BP. The maximum age of peat deposits exceeds 10 thousand years and is characteristic of the HP site with the maximum peat deposit depth. At the HPH and HH sites, the age is  $6780 \pm 100$  cal.yr BP and  $6580 \pm 110$  cal.yr BP, respectively; it correlates with the peat deposit depth at these sites. The youngest study site L is  $5740 \pm 90$  cal.yr BP.

The data (Figure 7) show that the peat deposits of all study sites are characterized by a high degree of homogeneity in botanical composition and are composed mainly of *Sphagnum* peat, with an admixture of herbaceous plants in some layers (sedge, *Scheuchzeria*, cotton grass). The exceptions are the bottom layers, in which cotton grass peat is deposited at the study site L, *scheuchzeria* peat at the study site HH, and wood peat at the study site HP. In the body of the deposit at different depths, there are rare, rather narrow layers of peat of other types: the sedge peat at the study site L (layer 80–90 cm) and the woody-herbal at the study site HP (layer 510–520 cm).

The results of the microscopic determination of the degree of decomposition (R) are given in Figure 8. The rate of decomposition of the main part of the peat deposit for all study sites ranges from 5 to 15%. The higher values are characteristic of the lower layers of the peat deposit at the study site HP (below 240 cm), where the rate of the decomposition varies between 5 and 25%. At all study sites, the trend of the growth of the decomposition rate with depth is observed; maximum values are noticed in the near-bottom layers. At the study site HP, with the highest peat deposit depth, the degree of decomposition reaches  $R = 35\text{--}45\%$ , in comparison with  $R = 30\text{--}35\%$  at the study site HPH, and  $R = 20\text{--}30\%$  at the study site HH. At the study site L, the decomposition rate is close to 35%. It should

be noted that at some study sites there are intermediate decomposition rate maximums:  $R = 30\%$  at 80–100 cm depth (the study sites HH and L) and at 210–220 cm depth (the study site HPH).

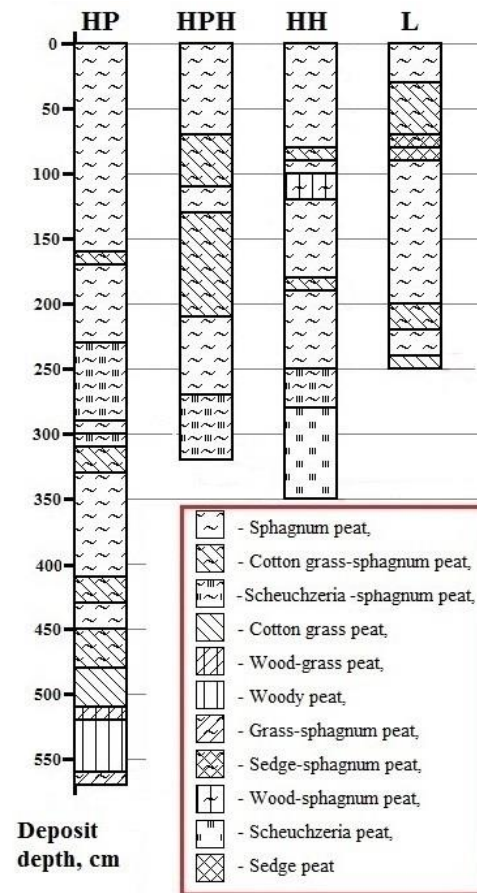


**Figure 7.** The botanical composition of peat deposits at the study sites: HP (hummock–pool complex); HPH (hummock–pool–hollow complex); HH (hummock–hollow complex); L (lawn).

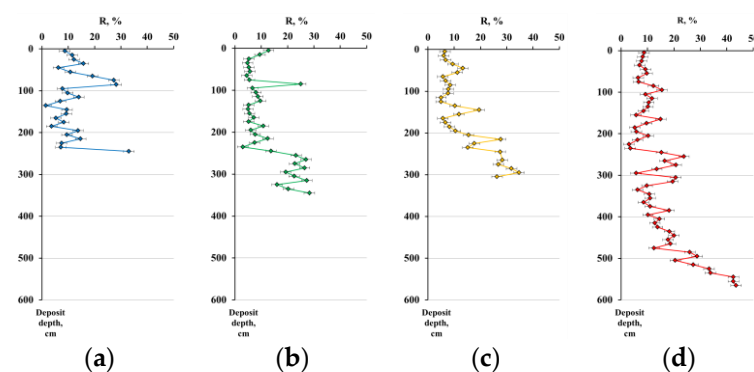


**Figure 8.** The degree of decomposition of peat at the study sites: (a) lawn; (b) hummock–hollow complex; (c) hummock–pool–hollow complex; (d) hummock–pool complex.

### 3.3.2. Physico-Chemical Characteristics of Peat Deposits

The study of the physical-chemical parameters of peat deposits (temperature, pH, mineralization, Red-Ox potential) was carried out in the upper layer (0–100 cm) due to the fact that the upper layers of peat deposits are most sensitive to external influences, and also correspond in each case to the current stage of the bog-forming process. The results are presented in Figure 9.

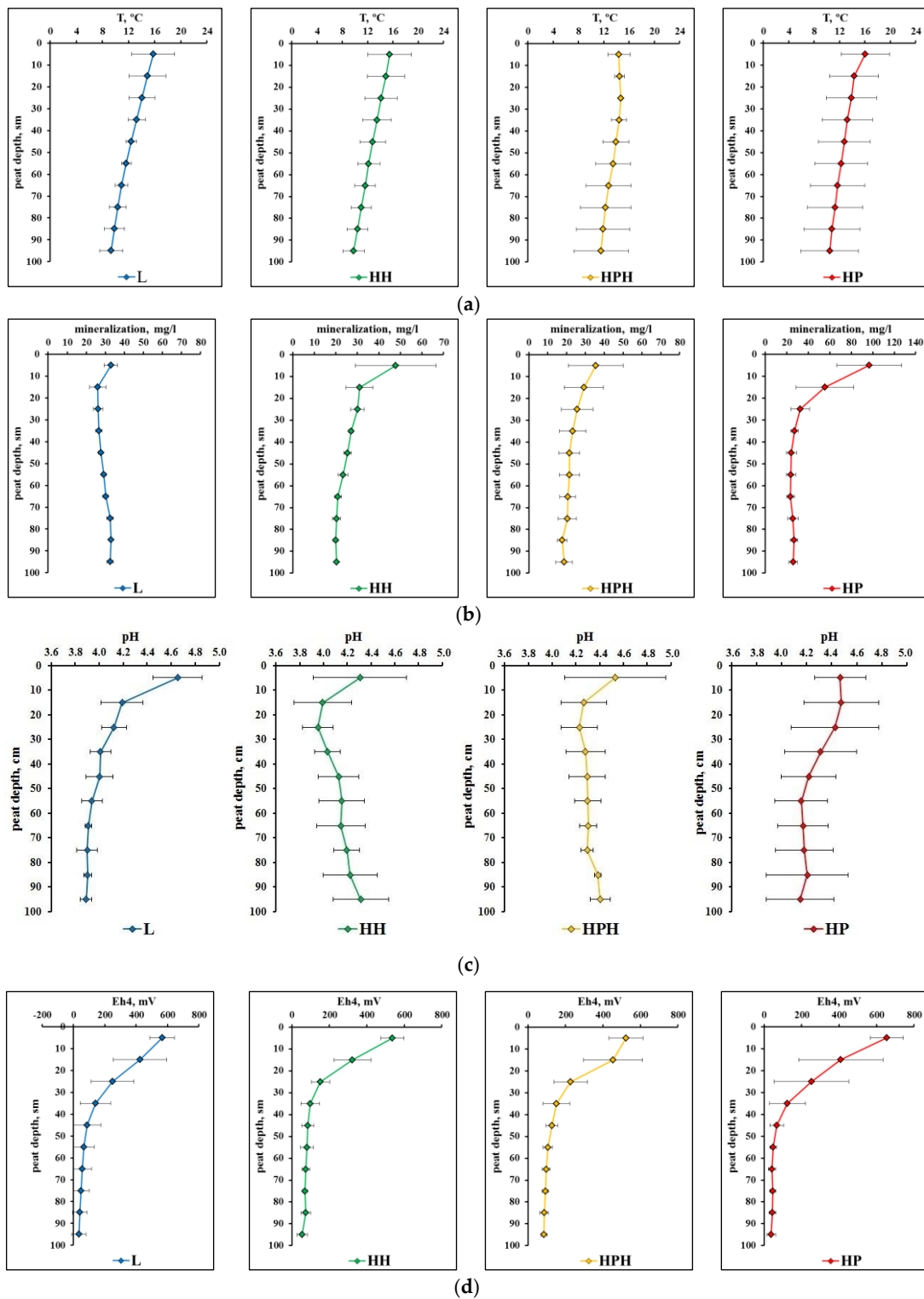


**Figure 9.** The dynamics of changes: (a) T, °C; (b) mineralization, mg/L; (c) pH; (d) Eh<sub>4</sub>, mV.: HP (hummock–pool complex); HPH (hummock–pool–hollow complex); HH (hummock–hollow complex); L (lawn).

The data obtained during the 2022 field season demonstrate that studied parameters are characterized by visible changes, both between study sites and seasons.

The peat deposit at study site L has the thinnest of all studied complex microlandscape peat deposit depths and is distinguished by the highest bog water table level (WTL) (Figure 4). The maximum temperature of the deposit is typical for the upper layer and is

$15.8 \pm 3.3$  °C. The temperature of the deposit is monotonically reduced with the depth to a minimum of  $9.3 \pm 1.8$  °C (layer 90–100 cm). The maximum temperature fluctuations during the warm period are observed on the layer 0–10 cm and do not exceed 8 °C.

The mineralization of pore water is unchanged with the depth of the deposit. Mean values vary from  $26 \pm 2.5$  to  $33 \pm 3.5$  mg/L.

The pH values range from  $3.89 \pm 0.05$  to  $4.65 \pm 0.21$ . The maximum values are characteristic for the surface layer and minimal for the layer of 90–100 cm. The study site L is characterized by a non-monotone reduction in pH value with the depth of the deposit. The maximum pH value reduction is observed in the acrotelm (0–40 cm).

The mean values of  $Eh_4$  vary between  $35 \pm 45$  and  $566 \pm 79$  mV by the depth of the deposit. The maximum values are noticed in the upper aerated layers of the deposit (acrotelm), and the minimum is in the layer of 80–100 cm. The maximum seasonal fluctuation amplitude is characteristic for the acrotelm zone (layers 10–20 and 20–30 cm) and reaches 300–400 mV. The change in the depth of the  $Eh_4$  value is a non-monotonic descending curve with the highest dynamics in the acrotelm (at depths of 0–40 cm) and minimal in the catotelm (deeper than 40 cm).

The temperature regime of the deposit at the study site HH is similar to that at the study site L, both in terms of the mean values and of the dynamic caused by the depth of the deposit. The maximum mean value is typical for the upper horizon and is  $15.5 \pm 3.5$  °C; the minimum is  $9.8 \pm 1.7$  °C (horizon of 90–100 cm). The maximum fluctuation amplitude during the warm period is also characteristic for the horizon of 0–10 cm, and is 8 °C. The mineralization of the pore water at the study site HH ranges from  $19.9 \pm 1.0$  to  $47.7 \pm 18.8$  mg/L. The maximum is observed in the layer of 0–10 cm and the minimum value is observed in the layer of 80–90 cm. The pore water mineralization curve can be divided into two sections. The first one is the upper (0–20 cm) zone of intense drop; the mean mineralization decreases from  $47.7 \pm 18.8$  to  $31.0 \pm 6.3$  mg/L. The second zone is the zone of smooth drop (20–100 cm); the mean mineralization decreases from  $31.0 \pm 6.3$  to  $19.9 \pm 1.0$  mg/L. The maximum amplitude of the seasonal variation is characteristic of the zone of intense run-off.

The pH values range from  $3.95 \pm 0.13$  to  $4.31 \pm 0.39$ . The pattern of the change in pH values with depth is characterized by the absence of pronounced dynamics. The upper layer (0–10 cm) is characterized by the maximum pH value ( $4.31 \pm 0.39$ ). There is a slight acidification of the peat, with the minimum value for this study site at a depth of 20–30 cm. Further, the pH values gradually increase with depth to the second maximum ( $4.31 \pm 0.23$ ) in the layer of 90–100 cm. The maximum amplitude of seasonal fluctuations is characteristic of the surface layer.

The  $Eh_4$  values range from  $55 \pm 28$  to  $535 \pm 63$  mV. The maximum of the  $Eh_4$  values is also characteristic of the acrotelm. The dynamics of changes by depth is similar to those at study site L. It should be noted that the seasonal fluctuations in the  $Eh_4$  values at this study site are minimal compared to other surveyed ones.

At the study site HPH, the following trends were revealed when measuring physico-chemical parameters. The temperature regime of the deposit has some differences. Firstly, this area is characterized by a weaker heating of the deposit in the summer (the maximum value is  $14.7 \pm 0.2$  °C); the entire acrotelm zone (0–40 cm) is characterized by the same temperature level from  $14.4 \pm 1.8$  to  $14.7 \pm 0.2$  °C. In the zone of catotelm, there is a gradual decrease in temperature values by the depth of the deposit to a minimum of  $11.6 \pm 4.3$  °C at the depth of 90–100 cm. The maximum amplitude of temperature fluctuations is characteristic of catotelm.

Changes in pore water mineralization with depth are similar to those at the HH study site. At the same time, the values at the study site HPH vary in a narrower range (from  $17.7 \pm 2.6$  to  $35.4 \pm 14.6$  mg/L). The maximum values of the mineralization are characteristic of the surface layer (0–10 cm). There is a gradual decrease in the specific electrical conduction (SEC) values by depth and its stabilization in the catotelm zone at the level of 17.7–21.5 mg/L.

The pH values range from  $4.23 \pm 0.08$  to  $4.53 \pm 0.43$ . The shape of the curve of pH values changing by depth is similar to the study site HH, but in a narrower range. The upper layer (0–10 cm) is characterized by the maximum pH value ( $4.53 \pm 0.43$ ); there is a slight acidification of the peat to the minimum value for this study site at a depth of 20–30 cm. The pH value gradually increases with depth to the second maximum ( $4.41 \pm 0.08$ ) in the layer of 90–100 cm. The maximum amplitude of seasonal fluctuations is also characteristic of the surface layer.

The Eh<sub>4</sub> values vary in the range of  $86 \pm 16$  to  $522 \pm 91$  mV. The maximum values, as well as at the study sites L and HH, were found in the upper layer of the acrotelm. The Eh<sub>4</sub> value decreases with depth of the deposit to the minimum at a depth of 90–100 cm.

The study site HP is characterized by the maximum thickness of the peat deposit (Figure 6), as well as the largest amplitude of WTL fluctuations (Figure 4). The temperature regime of the deposit is characterized by a maximum ( $16.1 \pm 3.8$  °C) in the upper layer and a gradual decrease in temperature values to a minimum ( $10.4 \pm 3.8$  °C) in the layer of 90–100 cm. Seasonal fluctuations of the deposit temperature have the highest values among all the studied sites and are observed over the entire range of the studied depths.

Changes in the pore water mineralization values by the deposit depth are similar to the study site HPH; however, the range of change is wider. Mean values vary from  $26.1 \pm 4.0$  to  $97 \pm 30.2$  mg/L. The pH values vary in the range of  $4.15 \pm 0.27$  to  $4.47 \pm 0.20$ . The maximum values are typical for the surface layer; the minimum values are observed for the layer of 90–100 cm. In the dynamics of changes with the depth in pH values is heterogeneous.

The average values of the Eh<sub>4</sub> by the depth of the deposit vary in the range of  $38 \pm 23$  to  $655 \pm 89$  mV. The maximum values are noted in the upper aerated layers (acrotelm); the minimum in the layers of 60–100 cm. The maximum seasonal amplitude of fluctuations is typical for the acrotelm zone (10–20 and 20–30 cm layers) and reaches 400–450 mV. Changes in the Eh<sub>4</sub> by the depth of the deposit represent a curve of non-monotonic decrease with the maximum dynamics in the acrotelm (at depths of 0–40 cm) and the minimum in the catotelm (deeper than 40 cm). It is also worth noting that the study site HP is characterized by the highest oxidation of the peat deposit in the acrotelm zone.

## 4. Discussion

### 4.1. Characteristics of the Components of Complex Microlandscapes

#### 4.1.1. Similarity and Difference in the Origin, Structure, and Properties of Peat Deposits

The radiocarbon age data (Table 1) confirm that selected study sites form a time scale row of the development of the ombrotrophic bog. According to the age hierarchy, the study sites could be arranged in the following order: (1) lawn (emerging hummock–hollow complex microlandscape) ( $5740 \pm 90$  cal.yr BP); (2) hummock–hollow complex microlandscape ( $6580 \pm 110$  cal.yr BP); (3) hummock–pool–hollow complex microlandscape ( $6780 \pm 100$  cal.yr BP); (4) hummock–pool complex microlandscape ( $10,460 \pm 130$  cal.yr BP). This is consistent with the spatial location of the study sites within the studied ombrotrophic bog massif (Figure 1) and with the spatial row of the central oligotrophic development of oligotrophic bogs proposed by Yurkovskaya [13]. In a similar row, studied sites are lined up according to the depth of peat deposits: from lawn to hummock–pool sites (Table 1). The botanical composition of the peat deposit (Figure 6) shows that the entire bog massif has developed as ombrotrophic since its formation. It is only on the hummock–pool complex that the lower layer (520–560 cm) is formed by eutrophic peat with a gradual change to wood-grass peat of transition type. This confirms the opinion that the area of the modern oligotrophic massif was originally covered by separate mesotrophic/eutrophic small mires. The researchers attribute this fact to the cooling, increased precipitation, and, related to this, the rise of groundwater at the beginning of the Atlantic period (5300–8830 years old). During this period, waterlogging was actively developing (the mire area increased up to 5–7 times), with the merging of numerous mesotrophic/eutrophic small mires associated with negative post-glacial relief and a fast transition to convex bogs [48–50]. This is

confirmed by the absence of eutrophic and mesotrophic peat at the base of peat deposits at younger sites (HH, HPH, L) (Figure 6).

As expected, the large difference in peat deposit depth between the central hummock–pool and edge lawn study sites creates heterogeneity in humidification (Figure 4). The central part of the massif is currently well drained, but in the past this site has passed all the geological stages of formation of the ombrotrophic bog [51], and the areas closer to the periphery are intermediate stages of this process. Currently, these territories go along the path of development of the central part of the bog and gradually «catch up» with its height. This is confirmed by the fact that the top layer of the weakly decomposed *Sphagnum* peat (with a decomposition rate not exceeding 20%) sometimes with mixtures of cotton grass and scheuchzeria, at the youngest section L, is only 260 cm, reaching 500 cm at the study site HP. This is well traced by the botanical composition of the peat deposit. The active accumulation of weakly decomposed oligotrophic peat (Figure 6) is explained by the fact that in the sub-boreal period (4500–2500 years ago) oligotrophic processes in the boreal zone had the maximum development [48–50].

It should be noted that the hydrological regime of all study sites shows a similar seasonal trend. The differences in bog water levels are mainly determined by the well differentiated microtopography (hummocks) of the site. The highest hummocks are found on the hummock–pool complex, which provides the lowest water level on average per season ( $-18.9 \pm 11.3$  cm). On the study site L, the ridges are almost not expressed, which explains the average water level close to the surface ( $-4.6 \pm 2.9$  cm). A similar interpretation is found in [30]. Changes in temperature conditions through the depth of the peat deposit are similar at all study sites and have close values of maximum and minimum values (Figure 8a). The maximum temperature range (up to 8 °C) is observed in the zone of fluctuation of the bog waters. The similarity of the peat deposit temperature regime along with the big differences in the magnitude of bog water level fluctuations is explained by the high humidity of the peat, even in the upper layers. The capillary rise of water due to the well-preserved structure of the plant residues maintains the high humidity of peat even when the bog water level decreases. It is interesting that seasonal variations in the temperature of the peat deposit are traced at the entire examined depth (up to 1 m). This seems to be due to the high humidity of the peat substrate, which ensures its thermal conductivity and the transfer of heat energy from the surface to the lower layers of the deposit. At the same time, the trend towards an increase in the magnitude of seasonal variations in the temperature of the deposit with a decrease in the mean water level is associated with a higher thermal capacity of the well-watered layers of peat deposit compared with more aerated ones. These results are in accordance with Kiselev et al. [52], where a similar trend was indicated when discussing the characteristics of the temperature regime of the drained and natural peat deposits of western Siberia.

The pH of peat deposits is considered to be an important factor in the development of bog ecosystems. The pH values of the acrotelm of all studied complex microlandscapes lie at the lower boundary of the middle acidic zone within pH 3.9–4.5 (Figure 8c), which is typical for ombrotrophic bogs. A marked decrease in pH occurs in the constant wetting zone (below the seasonal minimum of bog water level), which is explained by the stagnation of microbial processes under limited oxygen access. The seasonal variation in the reaction of the environment is not prominent in the permanently watered layers of the peat deposit; the maximum seasonal fluctuation of pH was detected in the surface layers of acrotelm on all study sites. It can be interpreted as a consequence of changes in dissolved carbon dioxide and organic acids concentration due to dilution of bog waters by atmospheric precipitation (during rainfall and heavy snowmelt) or concentration by evaporation (in hot and/or dry periods), considering that the botanical composition of the upper layers of all studied peat deposits is similar.

The oxidation-reduction regime of peat deposits is an important indicator determining the intensity and direction of oxidation-reduction processes. The Eh value quantifies the oxidation and reduction modes, which depend on a wide range of indicators, such

as aeration, humidity and composition of peat, microbiota activity, temperature, acidity, etc. [42,53]. The value of the  $Eh_4$  indicator gives a comprehensive view of the activity of the microbiota and the rate of degradation of the organic matter in the deposit. A contrast profile of oxidative-reducing conditions is characteristic of all studied peat deposits (Figure 8d). Moderate oxidative conditions of 400–600 mV are observed in the upper layers of the peat deposit (up to a depth of 10–20 cm) at all study sites. This is due to the high aeration of the upper layers. At the same time, the maximum  $Eh_4$  values are observed in the surface layer of the HP site, which corresponds to intensive oxidative conditions. It seems logical to attribute this to the lowest bog water level of the site peat deposit, as well as to the maximum mineralization of the bog waters compared to the deposits of the rest of the studied complex microlandscapes. The latter seems to be due to the peculiarities of the vegetation cover of the HP site, namely the largest number of higher vascular plants, the specificity of development of their root systems, and the quality of plant litter, which allows the localization of the mineral components of peat in the upper 10 cm layers.

There is a gradual transition to moderate oxidative conditions at the level of 200–400 mV (the lower part of the acrotelm) with depth and further, to a slight-reduction of the conditions at the level of 50–200 mV (in the catotelm). In general, the  $Eh_4$  variation profiles of the peat deposits are similar for all the study sites, further confirming their genetic unity.

Thus, the variation in the bog water levels, largely due to the development of the elements of microrelief (hummocks and mounds), is a key factor determining the functioning of the peat deposit, and, respectively, the speed of the formation of complex microlandscapes on all studied sites. The peripheral areas of the bog, permanently watered and without well-differentiated microtopography, are characterized by optimum conditions (hydrological and temperature) for peat-forming processes. The constant wetting of peat deposits leads to a minimum level of aeration of the upper layers, which slows down the decomposition of organic matter, contributing to its accumulation. Lowering the water levels from younger to more mature sites increases the area of aeration. This affects the transformation of the physical and chemical processes in it. At the same time, the preservation of the capillary structure of slightly decomposed peat seems to contribute to maintaining its high humidity even in the aerated layer, which inhibits microbiological activity and the degradation of peat even on the hummock–pool complex microlandscape. The latter claim requires further research.

#### 4.1.2. Similarity and Difference between Vegetation and Flora

The floristic list given in Table S1 includes 32 species: dwarf shrubs, herbaceous plants, the most widespread species of green and *Sphagnum* mosses, and lichens. They are all characteristic of ombrotrophic bogs [20]. The Venn diagram (Figure 10) shows a significant similarity in the flora of all sites studied. The 26 of the 32 species appear at all study sites. This was expected, because the oligotrophic conditions are maintained on all studied sites of complex microlandscapes.

The morphometric values of the tree layer change according to the stages of the bog formation process. There are separate strongly suppressed pines on study site L. The tree stand on the hummock–hollow complex is formed by *Pinus sylvestris* f. *willkommii*, while the tree layer is formed by higher and less light-demanding *Pinus sylvestris* f. *litwinowii* on older plots with relatively low water levels. As indicated by Abolin in reference [54], *Pinus sylvestris* f. *litwinowii* is characterized by a height of 3–5 m. The increment of trunks and branches does not exceed 5–8 cm per year. The crown is narrow, oval, or elongated. The length of the crown is 45–60% of the length of the trunk. *Pinus sylvestris* f. *willkommii* differs in height up to 3 m, more often 1.0–1.5 m. The trunk and branch growth is not high (up to 2–3 cm per year). The crown is elongated, covering up to 70% of trunk height. According to the morphometric values of the tree layer, except for crown density, the HH study site is significantly different from the HPH and HP study sites. The Mann–Whitney criterion confirms that the morphometric parameters of pine stands (height, diameter of the trunk,

and age of trees) significantly differ on the HH study site from the more mature and drier sites HPH and HP (Table 1).

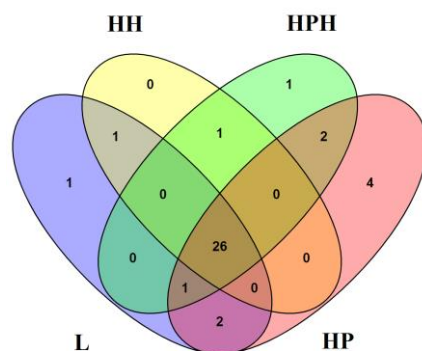


**Figure 10.** The Venn diagram showing the overlapping and individuality of flora of the studied complex microlandscapes: HP (hummock–pool complex); HPH (hummock–pool–hollow complex); HH (hummock–hollow complex); L (lawn). The Arabic figures in the diagram represent the number of species.

The projective cover of grasses, shrubs, and mosses does not significantly differ at the study sites (Figure 6). However, statistically significant differences in the height for shrubs have been identified (Figure 5). The dwarf shrub layer is the most developed on the study site HP. The spatial structure of the living vegetation cover is formed mainly by *Ledum palustre* and *Vaccinium uliginosum*, the projective cover of which reaches 50%. It is these species that show significant differences between the studied sites in the height of plants. The Mann–Whitney criterion confirms that the height of the *Ledum palustre* on the HP study site is significantly different from its height on the L and HH sites. The height of *Vaccinium uliginosum* on the same site differs from that of site L. The increase in the height of these two dwarf shrubs on the study site HP is accompanied by the appearance in the vegetation cover of *Vaccinium myrtillus*, and *Vaccinium vitis-idaea*. *Ledum palustre*, *Vaccinium uliginosum*, *V. vitis-idaea*, and *V. myrtillus* are species whose ecological optimum extends not only to bogs, but also to forest areas, i.e., the lowering of the water level and the formation of a tree canopy in the central part of the bog contribute to the development of coenopopulation, including these shrubs [55]. This is confirmed at the investigated sites. In addition, the Mann–Whitney criterion indicates differences in the height of some other shrubs. The height of the *Empetrum hermaphroditum* varies between HH and HPH sites, while the height of the *Andromeda polifolia* varies between HH and HP sites.

The spatial structure and morphometric indicators of herbs are similar for all study sites. The herbs layer of the study site L and of the hollows of the other study sites is characterized by a low percentage of projective cover of herbaceous plants due to morphological features of *Eriophorum vaginatum* and *Scheuchzeria palustris*; the main contribution to the spatial structure of the living vegetation cover of all study sites is made by large leaves of *Rubus chamaemorus* on the hummocks.

*Sphagnum* mosses are the environment-forming plants at all study sites. The percentage of projective coverage of *Sphagnum* mosses on study site L and HH reaches 100% of the area, even on the hummocks, in spaces with poor development of dwarf shrubs. In the central part of the bog, when the water level is lowered, the *Sphagnum* cover becomes more mosaic, and it is minimized on hummocks, where it is shadowed by trees and shrubs. The projective cover of true mosses exceeds the projective cover of *Sphagnum* mosses on some mounds at the HH and HP study sites. However, *Sphagnum* mosses have a leading environmental role within all complex microlandscapes.

Thus, we revealed notable differences in the spatial structure and morphometric characteristics of the vegetation cover of complex microlandscapes, due to the peculiarities of the peat deposit, despite the similarity of the floristic composition of the investigated sites and the predominance of *Sphagnum* mosses. Reduced water levels on well-differentiated

hummocks contribute to the development of perennial vascular plants and lead to the formation of a mosaic moss cover.

#### 4.2. Specificity of Relationships within Complex Microlandscapes

The generalization of the obtained data enabled the construction of the dendrogram, based on a set of ecosystem parameters shown in Figure 11. It clearly confirms that the investigated sites represent a spatiotemporal row of genetically connected intra-bog ecosystems.

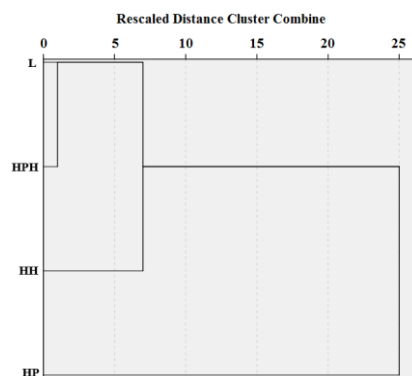


**Figure 11.** The dendrogram uses average linkage (between groups). The study sites were analyzed using hierarchical cluster analysis. HP (hummock–pool complex); HPH (hummock–pool–hollow complex); HH (hummock–hollow complex); L (lawn).

At the first stage of clustering, study sites L and HPH are combined. The study site HH is connected to this cluster at the next stage; as a result, the first cluster of three sites close by age is formed. The HP study site is joined at the third stage, forming the second cluster. This can probably be explained by the fact that the hummock–pool complex microlandscape of the studied bog has already entered the degradation stage, when the processes of bog formation are already fading out. In other complex microlandscapes of the studied bog, the peat formation process is predominant, although it has different speeds.

Thus, the selected complex microlandscapes correspond to all stages of the development of the bog, from the beginning of the formation to the transition to the degradation stage. It manifests in the structure and properties of both the peat deposit and the vegetation cover with a pronounced genetic unity.

The experimental data show that, despite the active processes of peat formation within the boundaries of the ecosystem as a whole, there is a question of the efficiency of carbon sequestration by mature complex microlandscapes. The open water mirror occupies its significant surface area, and the vegetation of high ridges is dominated by perennial vascular plants. This issue is particularly acute for boreal bogs. This is quite consistent with the basic thesis set out in reference [56] but requires further research.

#### 4.3. Specificity of Interactions of Complex Microlandscapes with External Factors

The main factors determining the water level regime of the bog, as researchers consider them, are the amount of precipitation and temperature [57–61]. As shown above, the water level determines the specific functioning of the peat deposit of complex microlandscapes, as well as the spatial structure of vegetation cover. Our results show that air temperature has a high influence (correlation coefficient was  $r = -0.818$ , at the significance level of  $p < 0.05$ ) on the bog water level regime of the studied bog (by regulating evaporation from the surface of the bog and evapotranspiration). The relationship of mean bog water level to precipitation was also significant but weaker (the correlation coefficient for all study sites was  $r = 0.520$ , at the significance level of  $p < 0.05$ ).

The generalization of the obtained data allows us to state that vegetation cover, especially higher vascular plants, plays an important role in the formation of a specific hydrothermal regime at the investigated sites. The correlation coefficients showed that the

relationship of mean seasonal bog water level and air temperature near the plant cover and the morphometric values of the trees (height, diameter) and dwarf shrubs (height of plants, projective cover) is strong and reciprocal (Table 3). The shade density has a much weaker influence on studied plants parameters (Table 3). A significant positive moderate relationship was found with the height of dominant species of dwarf shrubs. The projective cover shows a weak relationship with environmental factors.

**Table 3.** Relationship of morphometric values of higher vascular plants to parameters of the hydrothermal regime (Spearman rank correlations,  $n = 30$ ).

	Air Temperature Near the Plant Cover	Water Table Level	Shade Density
Height of Scots pine	0.864 *	−0.703 *	-
Diameter of Scots pine	0.912 *	−0.664 *	-
Height of Bog Rosemary	0.605 *	−0.702 *	0.352
Height of Blueberry	0.642 *	−0.604 *	0.422 *
Projective cover of dwarf shrub layer	−0.142	0.198	−0.103

\*Significant correlations are denoted with asterisks \* (at significance level of  $p < 0.05$ ).

Temperature variations at the different study sites are uneven during the warm season and vary in amplitude. Thus, at the beginning and in the end of the growing season, the air in the non-wooded study site L heats up worse. Its temperature is 1.0–1.6 °C lower, while in the study sites HPH and HP with the dense tree layer, on the contrary, it is warmer—the air temperature is higher, for 0.1–0.8 °C and for 0.5–1.3 °C, respectively. The warming of the air in late May and early June leads to a change in trends. The air over the studied non-wooded study site L begins to heat up more intensively. The temperature exceedance at the weather station is 1.1–1.4 °C. The air above the HPH and HP sites is cooler (1.0–3.0 °C and 1.6–3.6 °C, respectively). In [62], authors interpret this as follows: on sites with developed higher vascular plants, on the one hand, the moss layer is shadowed, reducing evaporation; on the other hand, the developed root system of trees and perennial dwarf shrubs actively extract water from the peat deposit, using it for transpiration. The development of the tree and dwarf shrub layers affects the warming of the living vegetation cover. The difference between living vegetation cover temperatures and air temperatures at the 2.0 m height is most pronounced on the treeless study site (L). The ground cover can stay 8.0–10.1 °C cooler at an air temperature close to 30 °C and 1.7–2.8 °C cooler at a temperature range of 10–20 °C. Similar results are shown in [62]. By the end of the warm season, the air and living vegetation cover temperatures are equal. For complex microlandscapes with a dense tree layer and developed dwarf shrub cover, the temperature difference is only visible in the temperature range above 20 °C. On such days, there is a pronounced heating of the living vegetation cover. The living vegetation cover temperature can be as high as 20.0–21.5 °C at the HPH site and 8.2–9.5 °C at the HP site above air temperature, as can be seen on the thermograms of the HPH and HP sites (Figure 3b).

The following interpretation of the relationships is logical. The formation of a specific thermal regime of complex microlandscapes within a studied bog massif is caused by the combined influence of the position of water levels and the specifics of the living vegetation cover. If on the L site, only the peat deposit (due to physical evaporation) regulates the thermal regime of the ecosystem, then, in the tree covered areas, the tree stand becomes actively involved in the formation of not only the hydrological regime, but also the thermal regime. The increased air temperature seems to increase the physical evaporation from the surface of the wet peat deposit; the dense tree layer contributes to the retention of moisture, especially when wind blows are reduced.

## 5. Conclusions

Complex studies have confirmed the hypothesis that the selected complex microlandscapes of the ombrotrophic bog massif are interconnected, are at successive stages of morphogenesis of the bog, and possess a specific set of parameters and characteristics.

It was determined that the regulation of the microclimate within complex microlandscapes, with equal inputs, is carried out by the system of “living vegetation cover-peat deposits”. Moreover, the older the complex microlandscape, the more pronounced influence on the microclimate has the tree and perennial dwarf shrub layers. Morphometric indicators of perennial dwarf shrubs (the bog rosemary and blueberries in particular) can serve as indicators of the stages of development of the ombrotrophic convex bog. When studying the specifics of interconnections of complex microlandscapes with external factors, it was found that the relationship with the temperature factor is higher than with the precipitation factor.

In the course of the development of the bog, the self-regulation processes of individual complex microlandscapes are disrupted, as evidenced by an increase in the amplitude of temperature and the water levels, as well as key physico-chemical parameters (oxidative reduction potential and mineralization) of peat deposits. These disturbances were observed in the studied bog massif at the site of the hummock–pool complex microlandscape, which has the maximum age and maximum depth of the deposit. This destabilization is due to changes in vegetation cover in particular. The coverage of *Sphagnum* mosses is reduced; species that inhibit evaporation from the surface of the peat deposit, vascular perennial plants, are actively developing, providing active evapotranspiration processes that lower the bog water level. This results in a gradual, slow conversion of the physico-chemical processes in the deposit, from the storage of organic matter to the degradation of peat biomass. The processes of destruction of organic matter are still rather weak at this stage of the existence of the hummock–pool microlandscape. This is confirmed through data on the decomposition rate and is probably due to the botanical composition of the active layer of the peat deposit.

**Supplementary Materials:** The following supporting information can be downloaded at: <https://www.mdpi.com/article/10.3390/quat7020019/s1>, Table S1: Projective cover of dwarf shrub, grass, moss, and lichens layers at the studied bog massif (%).

**Author Contributions:** Conceptualization, T.P., I.Z. and A.S.; methodology, A.O.; software, T.P. and A.S.; validation, S.S. and I.Z.; formal analysis, A.O.; writing—original draft preparation, T.P., A.S. and I.Z.; writing—review and editing, S.S. and A.O. All authors have read and agreed to the published version of the manuscript.

**Funding:** This research was funded by the Ministry of Education and Science of the Russian Federation, project number 122011400386-6, “Features of Formation and Diagenesis of Organic Matter in the Conditions of Wetland Ecosystems of the Arctic Zone of the Russian Federation”.

**Data Availability Statement:** The raw data supporting the conclusions of this article will be made available by the authors on request.

**Conflicts of Interest:** The authors declare no conflicts of interest. The funders had no role in the design of the study; in the collection, analysis, or interpretation of data; in the writing of the manuscript; or in the decision to publish the results.

## References

1. Montoro Girona, M.; Gauthier, S.; Morin, H.; Bergeron, Y. *Boreal Forests in the Face of Climate Change-Sustainable Management*; Springer Nature: Cham, Switzerland, 2023; 837p. [[CrossRef](#)]
2. Helbig, M.; Waddington, J.M.; Alekseychik, P.; Amiro, B.; Aurela, M.; Barr, A.G.; Black, T.A.; Carey, S.K.; Chen, J.; Chi, J.; et al. The biophysical climate mitigation potential of boreal peatlands during the growing season. *Environ. Res. Lett.* **2020**, *15*, 104004. [[CrossRef](#)]
3. Glebov, F.Z. *Relationship between Forest and Swamp in the Taiga Zone*; Science, Siberian Branch: Novosibirsk, Russia, 1988; 184p. (In Russian)
4. Yurkovskaya, T.K. The relationship of taiga forests and swamps in space and time. *Proc. Samara Sci. Cent. Russ. Acad. Sci.* **2012**, *14*, 1416–1419. (In Russian)
5. Sjöberg, K.; Lars, E. Mosaic Boreal Landscapes with Open and Forested Wetlands. *Ecol. Bull.* **1997**, *46*, 48–60.
6. Kuuluvainen, T.; Aapala, K.; Ahlroth, P.; Kuusinen, M.; Lindholm, T.; Sallantausta, T.; Siitonen, J.; Tukka, H. Principles of Ecological Restoration of Boreal Forested Ecosystems: Finland as an Example. *Silva Fenn.* **2002**, *36*, 409–422. [[CrossRef](#)]

7. Heiskanen, L.; Tuovinen, J.-P.; Vekuri, H.; Räsänen, A.; Virtanen, T.; Juutinen, S.; Lohila, A.; Mikola, J.; Aurela, M. Meteorological responses of carbon dioxide and methane fluxes in the terrestrial and aquatic ecosystems of a subarctic landscape. *Biogeosciences* **2023**, *20*, 545–572. [[CrossRef](#)]
8. Bhatti, J.S.; Tarnocai, C. Influence of Climate and Land Use Change on Carbon in Agriculture, Forest, and Peatland. In *Ecosystems across Canada in Soil Carbon Sequestration and the Greenhouse Effect*, 2nd ed.; Lal, R., Follett, F.R., Eds.; Soil Science Society of America: Madison, WI, USA, 2009; Volume 57. [[CrossRef](#)]
9. Bhatti, J.; Jassal, R.; Black, T.A. Decarbonization of the Atmosphere: Role of the Boreal Forest Under Changing Climate. In *Recarbonization of the Biosphere*; Lal, R., Lorenz, K., Hüttl, R., Schneider, B., von Braun, J., Eds.; Springer: Dordrecht, The Netherlands, 2012; pp. 203–228. [[CrossRef](#)]
10. Nikiforova, L.D. Some issues of environmental change and peat formation in the north of the Russian Plain. *Swamps Eur. North USSR Struct. Genes. Dyn.* **1980**, *66*, 155–177. (In Russian)
11. Lepin, L.Y. Peat fund of the Karelian ASSR. In *Peat Cadastre of the RSFSR: Karelian ASSR*; The Institute of Biology of the Karelian Branch of the Academy of Sciences of the USSR: Nedra, Moscow, 1957; pp. 5–25. (In Russian)
12. Yurkovskaya, T.K. *Geography and Cartography of Mire Vegetation of the European Russia and Neighbouring Territories*; Publishing House of the Komarov Botanical Institute: Saint Petersburg, Russia, 1992; 256p. (In Russian)
13. Yurkovskaya, T.K. Types of bog massifs on an overview map of the vegetation cover of the forest zone of the European part of the USSR. In *Types of Swamps of the USSR and Principles of Their Classification*; Nauka, Leningrad Branch: Leningrad, Russia, 1974; pp. 57–62. (In Russian)
14. Kuhry, P.; Turunen, J. The Postglacial Development of Boreal and Subarctic Peatlands. In *Boreal Peatland Ecosystems*; Wieder, R.K., Vitt, D.H., Eds.; Springer: Berlin, Germany, 2006; 436p.
15. Smagin, V.A.; Noskova, M.G.; Antipin, V.K.; Boychuk, M.A. Diversity and phytosociological role of mosses in mires of south-western Arkhangelsk region and adjacent territories. *Trans. Karelian Res. Cent. Russ. Acad. Sci.* **2017**, *1*, 75–96. (In Russian) [[CrossRef](#)]
16. Yu, Z.; Beilman, D.W.; Frolking, S.; MacDonald, G.M.; Roulet, N.T.; Camill, P.; Charman, D.J. Peatlands and Their Role in the Global Carbon Cycle. *EOS Trans.* **2011**, *92*, 97–98. [[CrossRef](#)]
17. Yu, Z. Northern peatland carbon stocks and dynamics: A review. *Biogeosciences* **2012**, *9*, 4071–4085. [[CrossRef](#)]
18. Jensen, M.; Demidov, I.N.; Larsen, E.; Lyså, A. Weichselian glaciers, lakes and sea level in the Arkhangelsk region: Correlation potential and challenges. *Correl. Pleistocene Events Russ. North* **2006**, *44*–45.
19. Panova, N.; Antipina, T.; Jankovska, V.; Panova, N.; Yankovska, V. Holocene history of the environment and development of bogs on the eastern slope of the Polar and Pre-Polar Urals. *Environ. Dyn. Glob. Clim. Chang.* **2010**, *1*, 8. [[CrossRef](#)]
20. Katz, N.Y. *Types of Bogs of the USSR and Western Europe and Its Geographical Distribution*; State Publishing House of Geographical Literature: Moscow, Russia, 1948; 318p. (In Russian)
21. Halsey, L.A.; Vitt, D.H.; Gignac, L.D. *Sphagnum*-dominated peatlands in North America since the Last Glacial Maximum: Their occurrence and extent. *Bryologist* **2000**, *103*, 334–352. [[CrossRef](#)]
22. Almquist-Jacobson, H.; Foster, D. Towards an integrated model for raised-bog development: Theory and field evidence. *Ecology* **1995**, *76*, 161–174. [[CrossRef](#)]
23. Couwenberg, J.; Joosten, H. Self-Organization in Raised Bog Patterning: The Origin of Microtope Zonation and Mesotope Diversity. *J. Ecol.* **2005**, *93*, 1238–1248. [[CrossRef](#)]
24. Runkle, B.; Wille, C.; Gazovic, M.; Wilmking, M.; Kutzbach, L. The surface energy balance and its drivers in a boreal peatland fen of northwestern Russia. *J. Hydrol.* **2014**, *511*, 359–373. [[CrossRef](#)]
25. Wu, J.; Roulet, N.; Moore, T.; Lafleur, P.; Humphreys, E. Dealing with microtopography of an ombrotrophic bog for simulating ecosystem-level CO<sub>2</sub> exchanges. *Ecol. Model.* **2011**, *222*, 1038–1047. [[CrossRef](#)]
26. Gorham, E. Northern peatlands: Role in the carbon cycle and probable responses to climatic warming. *Ecol. Appl.* **1991**, *1*, 182–195. [[CrossRef](#)]
27. Foster, D.R.; Wright, H.E., Jr. Role of Ecosystem Development and Climate Change in Bog Formation in Central Sweden. *Ecology* **1990**, *71*, 450–463. [[CrossRef](#)]
28. Gorham, E. The Development of Peat Lands. *Q. Rev. Biol.* **1957**, *32*, 145–166. [[CrossRef](#)]
29. Mäkilä, M.; Säavuori, H.; Grundström, A.; Suomi, T. *Sphagnum* decay patterns and bog microtopography in south-eastern Finland. *Mires Peat* **2018**, *21*, 13. [[CrossRef](#)]
30. Shi, X.; Thornton, P.; Ricciuto, D.; Hanson, P.; Mao, J.; Sebestyen, S.; Griffiths, N.; Bisht, G. Representing northern peatland microtopography and hydrology within the Community Land Model. *Biogeosciences* **2015**, *12*, 6463–6477. [[CrossRef](#)]
31. Kokkonen, N.; Laine, A.M.; Männistö, E.; Mehtätalo, L.; Korrensalo, A.; Tuittila, E.-S. Two Mechanisms Drive Changes in Boreal Peatland Photosynthesis Following Long-Term Water Level Drawdown: Species Turnover and Altered Photosynthetic Capacity. *Ecosystems* **2022**, *25*, 1601–1618. [[CrossRef](#)]
32. Dendievel, A.-M.; Argant, J.; Dietre, B.; Delrieu, F.; Jouannic, G.; Lemdahl, G.; Mennessier-Jouannet, C.; Mille, P.; Haas, J.N.; Cubizolle, H. Multi-proxy study of the Pialeloup Bog (SE Massif Central, France) reveals long-term human environmental changes affecting peat ecosystems during the Holocene. *Quat. Int.* **2022**, *636*, 118–133. [[CrossRef](#)]
33. The Weather and Climate. Available online: <http://www.pogodaiklimat.ru> (accessed on 15 April 2023).

34. Markov, M.L. *Long-Term Changes in the Elements of the Water Balance at Water Balance and Bog Stations: Scientific and Applied Reference Book*; OOO "RIAL": St. Petersburg, Russia, 2021; 202p. (In Russian)
35. Kuznetsov, O.L. Diversity of mire massif types in the boreal zone of European Russia. *IOP Conf. Ser. Earth Environ. Sci.* **2018**, *138*, 012011. [CrossRef]
36. Google Maps. Available online: <https://www.google.com/maps/@64.5340228,40.5630513,13z> (accessed on 15 April 2023).
37. Stankov, S.S. *Identification Guide of Higher Plants of the European Part of the USSR*, 2nd ed.; Soviet Science: Moscow, Russia, 1957; 741p. (In Russian)
38. Borisova, M.A.; Bogachev, V.V. *Geobotanics*; Yaroslavl State University Publishing House: Yaroslavl, Russia, 2009; 160p. (In Russian)
39. Noskova, M.G. *Field Identification Guide of Sphagnum Mosses*; Akvarius: Tula, Russia, 2016; p. 112. (In Russian)
40. Ignatov, M.S.; Ignatova, E.A. *Moss Flora of the Middle European Russia. Volume 2: Fontinalaceae-Amblystegiaceae*; KMK Scientific Press Ltd.: Moscow, Russia, 2003; pp. 609–944. (In Russian)
41. Ushakov, A.I. *Forest Inventory and Forest Management: Training Manual*; MGTU named after N.E. Bauman: Moscow, Russia, 1997; 176p. (In Russian)
42. Zubov, I.N.; Orlov, A.S.; Selyanina, S.B.; Zabelina, S.A.; Ponomareva, T.I. Redox potential and acidity of peat are key diagnostic physicochemical properties for the stratigraphic zones of a boreal raised bog. *Mires Peat* **2022**, *28*, 5. [CrossRef]
43. Urquhart, C.; Gore, A.J.P. The redox characteristics of four peat profiles. *Soil Biol. Biochem.* **1973**, *5*, 659–672. [CrossRef]
44. Kats, N.Y.; Kats, S.V.; Skobeeva, E.I. *Atlas of Plant Residues in Peat*; Nedra: Moscow, Russia, 1977; p. 371. (In Russian)
45. Zaretskaya, N.E.; Shevchenko, N.V.; Simakova, A.N.; Sulerzhitsky, L.D. Chronology of the North Dvina River delta development over the Holocene. *Geochronometria* **2011**, *38*, 116–127. (In Russian) [CrossRef]
46. Reimer, P.; Austin, W.; Bard, E.; Bayliss, A.; Blackwell, P.; Bronk Ramsey, C.; Butzin, M.; Cheng, H.; Edwards, R.L.; et al. The IntCal20 Northern Hemisphere Radiocarbon Age Calibration Curve (0–55 cal kBP). *Radiocarbon* **2020**, *62*, 725–757. [CrossRef]
47. Landau, S.; Everitt, B.S. *A Handbook of Statistical Analyses Using SPSS*; Chapman & Hall/CRC Press LLC: Boca Raton, FL, USA, 2004; 337p.
48. Tikhonravova, Y.V.; Slogoda, E.A.; Rogov, V.V.; Butakov, V.I.; Lupachev, A.V.; Kuznetsova, A.O.; Simonova, G.V. Heterogeneous ices in ice wedges structure on the Pur-Taz interfluvial peatlands of the North of West Siberia. *Ice Snow* **2020**, *60*, 225–238. [CrossRef]
49. Ashkepkova, A.; Semikolennykh, A. Sediments of swamps and caves of the Pinezh karst massif (Arkhangelsk region) as an indicator of changes of the natural environment in the Pleistocene–Holocene. In Proceedings of the Speleology and Speleology, V International Correspondence Conference, Naberezhnye Chelny, Russia, 29 November 2014; pp. 92–98. (In Russian)
50. Yurkovskaya, T. Main latitudinal and longitudinal characters of Russian mire vegetation. *Proc. IAVS Symp.* **2000**, 130–132.
51. Yurkovskaya, T.K. Peatlands of the taiga North-East of European Russia. *Bot. Zhurnal* **2021**, *106*, 211–228. [CrossRef]
52. Kiselev, M.V.; Dyukarev, E.A.; Voropay, N.N. The temperature characteristics of biological active period of the peat soils of Bakchar swamp. *IOP Conf. Ser. Earth Environ. Sci.* **2018**, *107*, 012032. [CrossRef]
53. Tokarz, E.; Urban, D. Soil Redox Potential and Its Impact on Microorganisms and Plants of Wetlands. *J. Ecol. Eng.* **2015**, *16*, 20–30. [CrossRef]
54. Abolin, R.I. Swamp forms of pine *Pinus sylvestris* L. *Ann. Bot. Mus. Acad. Sci.* **1915**, *15*, 62–84. (In Russian)
55. Kiseleva, K.V.; Novikov, V.S.; Mayorov, S.R. *Flora of Central Russia. Field Guide*; Phytos XXI: Moscow, Russia, 2019; 544p. (In Russian)
56. Słowińska, S.; Słowiński, M.; Marcisz, K.; Lamentowicz, M. Long-term microclimate study of a peatland in Central Europe to understand microrefugia. *Int. J. Biometeorol.* **2022**, *66*, 817–832. [CrossRef] [PubMed]
57. Davis, K.T.; Dobrowski, S.Z.; Holden, Z.A.; Higuera, P.E.; Abatzoglou, J.T. Microclimatic buffering in forests of the future: The role of local water balance. *Ecography* **2019**, *42*, 1–11. [CrossRef]
58. Bridgham, S.; Pastor, J.; Updegraff, K.; Malterer, T.J.; Johnson, K.; Harth, C.; Chen, J. Ecosystem control over temperature and energy flux in northern peatlands. *Ecol. Appl.* **1999**, *9*, 1345–1358. [CrossRef]
59. Chen, J.; Bridgham, S.; Keller, J.; Pastor, J.; Noormets, A.; Weltzin, J.F. Temperature responses to infrared-loading and water table manipulations in peatland mesocosms. *J. Integr. Plant Biol.* **2008**, *50*, 1484–1496. [CrossRef] [PubMed]
60. Zarzycki, J.; Skowera, B.; Zając, E. Microclimate and Water Conditions of an Extracted and Natural Raised Bog. *J. Ecol. Eng.* **2020**, *21*, 115–123. [CrossRef]
61. Rietkerk, M.; Dekker, S.C.; Wassen, M.J.; Verkroost, A.W.; Bierkens, M.F. A putative mechanism for bog patterning. *Am. Nat.* **2004**, *163*, 699–708. [CrossRef]
62. Linkevičienė, R.; Šimanauskienė, R.; Kibirkštis, G.; Grigaitė, O.; Taminskas, J. Hydrological and botanical techniques of raised bog and its methods in situ and remote sensing. *J. Hydrogaitė* **2023**, *617*, 129119. [CrossRef]

**Disclaimer/Publisher's Note:** The statements, opinions and data contained in all publications are solely those of the individual author(s) and contributor(s) and not of MDPI and/or the editor(s). MDPI and/or the editor(s) disclaim responsibility for any injury to people or property resulting from any ideas, methods, instructions or products referred to in the content.